THE AMERICAN MINERALOGIST, VOL. 48, JANUARY–FEBRUARY, 1963

XENOLITHS AND XENOCRYSTS FROM LAVAS OF THE KERGUELEN ARCHIPELAGO

J. L. TALBOT, B. E. HOBBS, H. G. WILSHIRE[1] AND T. R. SWEATMAN, *Dept. of Geology, Univ. of Adelaide, Adelaide, South Australia, Dept. of Geology, Univ. of Sydney, Sydney, New South Wales, Dept. of Geophysics, Australian National Univ., Canberra, A.C.T., C.S.I.R.O. Div. of Soils. Clay Min. Section, Adelaide.*

ABSTRACT

Ultramafic xenoliths in basalts and related rocks from Kerguelen are shown to have a metamorphic fabric. Olivines from the xenoliths have a wider range of composition than hitherto reported. Many of the large discrete olivine grains in basalts show chemical and textural similarities with those of the xenoliths and it is concluded that much of the olivine found in the basalts is derived from the xenoliths. Olivines which have crystallized from the magma differ from the xenocrysts in composition and texture. Partial analyses of 39 olivines show a marked regularity of variation of Ni and Mn with Fe content.

INTRODUCTION

The Kerguelen Archipelago is a group of volcanic islands in the Southern Indian Ocean encompassing an area approximately 120 miles N-S and 92 miles E-W and is located on a broad ridge on the ocean floor.

Geological studies of these islands include those of de La Rue (1932), who gives an extensive bibliography, and Edwards (1938). These studies show that the islands are predominantly basalt with minor trachyte and phonolite, a typical olivine basalt suite. Minor fluviatile beds, some with lignite, are interlayered with the volcanic rocks. Intrusive rocks of similar chemical composition to the volcanic rocks are present on some parts of the main island. Xenoliths of igneous material, generally ultrabasic, are abundant in some lava flows. Edwards (1938) did not consider the xenoliths in detail, and in view of the attention which has subsequently been paid to xenoliths in basalt it was felt that further study of material from Kerguelen was warranted.

The rocks studied were collected by members of the British, Australian and New Zealand Antarctic Research Expedition of 1929–1930 and were described by Edwards (1938). The specimens are housed in the Mawson Institute for Antarctic Research in the University of Adelaide, and the numbers referred to in the text are the BANZARE numbers allotted by Mawson and correspond to those used by Edwards.

Author responsibilities are as follows: J. L. Talbot, mineralogy and chemistry; B. E. Hobbs, microfabric analysis; H. G. Wilshire, petrology; T. R. Sweatman, analytical techniques and data. The overall interpretation is the result of collaboration of all of the authors.

[1] Present address: U. S. Geol. Survey, Paducah, Kentucky.

General Description of Xenoliths

The most common type of xenolith in the basaltic rocks is peridotite but pyroxenite and gabbro also occur. Xenoliths vary from nearly pure dunite through peridotite and feldspathic peridotite to gabbro. Biotite-hornblende pyroxenites and related xenoliths are largely restricted to trachybasalt host rocks but some have been reported as occurring in basalts (de La Rue, 1932, p. 124). Many of the xenoliths are traversed by macroscopically visible basalt veinlets, and in thin section many microscopic veinlets are seen to penetrate the xenoliths along irregular fractures or grain boundaries. Such veinlets pass laterally into, or are altered to, patches of clay, carbonate and zeolite.

Peridotite. Peridotite xenoliths consist of varying proportions of olivine, green diopsidic clinopyroxene, orthopyroxene, plagioclase and spinel. Phlogopite is a rare constituent. Brown spinel is not common, but a green variety is abundant in feldspathic peridotites. The fabric is granoblastic with all the principal constituents occurring as interlocking, generally equidimensional grains. Rare grains of clinopyroxene are interstitial to or molded onto other mineral grains. More commonly, spinel is concentrated in intergranular mosaics to be described below. Some grains of olivine, orthopyroxene and clinopyroxene show crystal faces, but these interlock perfectly with adjacent anhedral grains. Thin exsolution lamellae of orthopyroxene in clinopyroxene and of clinopyroxene in orthopyroxene are common. In some thin sections plagioclase encloses oriented rods of green spinel, but more commonly irregular granules of spinel are located along fractures in the feldspar.

Macroscopically, peridotite xenoliths exhibit a wide range of average grain size, but only rarely does this variation produce an indistinct lamination within a single xenolith. Rare lenticular concentrations of spinel in fine-grained, granular bands give rise to a layered structure which is indistinct in hand specimen, but which is prominent in thin section. The granular bands do not exceed 4 mm in width and separate coarser bands which average about 10 mm in width. Alignment of elongate spinels in granular bands is sometimes strong enough to give a macroscopic lineation, but other minerals even when elongate do not show any preferred orientation.

Minerals exposed at xenolith margins have commonly reacted with the host rock, and the effects observed include:

1) conversion of orthopyroxene to a granular mosaic of olivine, 2) normal zoning of olivine, 3) conversion of clinopyroxene to a spongy material riddled with minute glass (?) inclusions, 4) conversion of translucent spinel to an opaque ore, and 5) fusion of plagioclase.

Clinopyroxene of the xenoliths has commonly acted as a nucleus for precipitation of salite from the host basalt.

Gabbro. With increasing plagioclase the peridotites grade into gabbros which consist of olivine, clinopyroxene, plagioclase and green spinel with minor orthopyroxene. The fabric is granoblastic with most constituent minerals interlocking along irregular boundaries; poikilitic fabric is entirely lacking and few grains show any elongation. Spinel may be enclosed as oriented rods in plagioclase or irregularly arranged granules in olivine and pyroxene, but it is most common along grain boundaries where it is intergrown with a fine-grained mosaic of clinopyroxene and olivine. Some plagioclase grains appear to be progressively zoned but the observed extinction effects may be strain shadows as they are irregular and other minerals are unzoned. Trains of minute spinels in olivine and pyroxene are possibly the result of exsolution. Thin exsolution lamellae of orthopyroxene occur in clinopyroxene grains.

Pyroxenite. Pyroxenites consist largely of slightly pleochroic, gray-green to yellowish clinopyroxene (β 1.692–1.694 $2V_Z = 52°58°$), strongly pleochroic hypersthene and a little olivine. Local intergrowths of clinopyroxenes resemble the harrisitic structure described by Wager *et al.* (1960), but there is no constancy of orientation within individual xenoliths. The fabric of these xenoliths is commonly granoblastic but some clino-

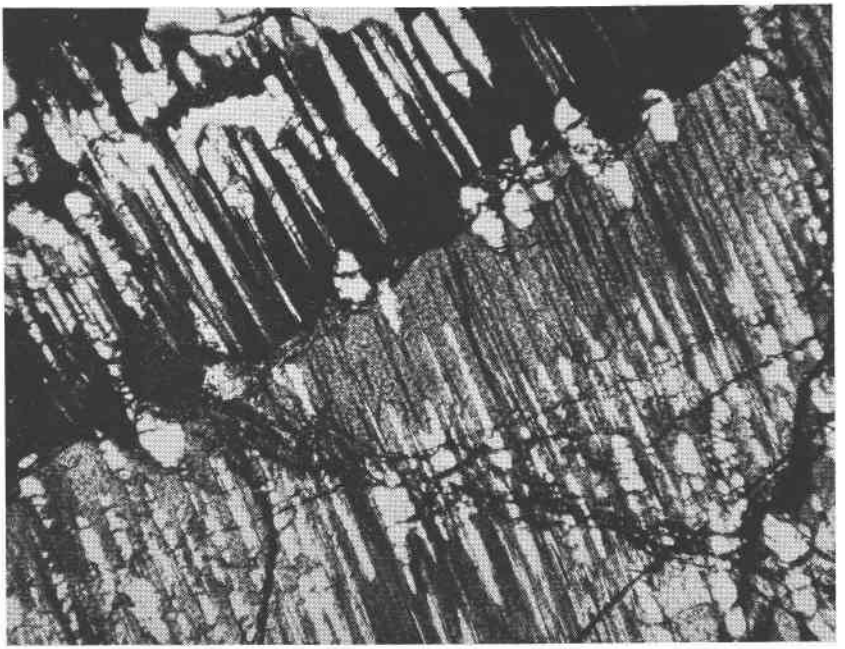

FIG. 1. Kink plane in orthopyroxene. Exsolution lamellae of clinopyroxene appear white in photograph. Crossed polars (K31B). Width of area 2.9 mm.

pyroxenes show marked elongation and are euhedral. Hypersthene occurs as anhedral grains interlocking with clinopyroxene, as stumpy lamellae parallel to {100} of the host clinopyroxene (see Brothers, 1960, p. 17 for complete orientation data) and as vaguely defined patches along fractures in clinopyroxene. A striking and common feature of hypersthene lamellae in clinopyroxene is the inter-connection of lamellae to produce hook- and U-shaped intergrowths (Fig. 1). Some clinopyroxene grains show progressive normal zoning, a zoned schiller structure with oriented inclusions (unidentified) restricted to cores of grains, or oriented rods of spinel. Diallage parting is well developed in some grains.

Marginal reactions of the xenoliths have produced broad rims of turbid clinopyroxene riddled with minute inclusions. Although hypersthene lamellae are abundant in the clinopyroxenes, they could not be identified in the reaction rim nor could any reaction product be attributed to them. A thin rim of clean pyroxene identical with that of the host rock is generally found at the outer margins of the xenoliths.

Biotite-hornblende pyroxenites. ("Hornblende Peridotite," Edwards, 1938). These xenoliths consist of pleochroic amphibole (X = deep yellow green; Y = brownish green; Z = olive green), biotite, colorless to slightly pleochroic clinopyroxene, olivine, orthopyroxene, apatite and magnetite. Large, euhedral apatite grains are commonly found as inclusions in pyroxene and amphibole within xenoliths. Edwards (1938, p. 89) stated that apatite is a decomposition product of turbid amphibole or of amphibole which has been replaced by magnetite and clinopyroxene, but this association is not constant and the apatite associated with decomposed amphibole may represent original inclusions. Apatite is also abundant as original constituents in similar xenoliths described by Frechen (1948), Holmes and Harwood (1937) and Wilshire and Binns (1961). Magnetite occurs as interstitial grains and as inclusions in amphibole and clinopyroxene. Rare euhedral crystals of sphene occur in some xenoliths. Clinopyroxene may contain exsolution lamellae of orthopyroxene parallel to {100} and is characterized by diallage parting. In some cases, hypersthene, occurring as discrete grains, contains exsolution lamellae of clinopyroxene.

Where the proportion of amphibole and biotite is high they occur as large irregular plates poikilitically enclosing other constituents; where low, these constituents are interstitial and pyroxene and olivine interlock to form a hypidiomorphic-granular or allotrimorphic-granular fabric. Unlike the peridotite and pyroxenite examples, the constituents of these xenoliths exhibit well developed crystal faces against interstitial zeolites within the xenolith. The same feature occurs where the xenolith

is disaggregated and penetrated by the host rock or by veinlets of secondary minerals originating in the host rock. Along the margins of some xenoliths, the constituent minerals form a loose-knit aggregate of well formed crystals which grades, toward the xenolith core, into a solid mesh of interlocking, anhedral grains.

Reactions at xenolith margins consist of a darkening of amphibole and biotite or conversion to very finely divided material consisting in part of opaque minerals. Greenish gray clinopyroxene has replaced the original clinopyroxene. The replacement is very patchy and has in many cases proceeded along cleavage fractures of the original grain. The same replacement, accompanied by development of crystal faces, is found in the centers of xenoliths along veinlets and interstitial patches of zeolite. Identical greenish-gray pyroxene occurs as a groundmass constituent of the host rocks, and development of crystal faces on originally anhedral grains may have been caused by precipitation from the host magma. This is analogous to formation of salite rims on clinopyroxene xenocrysts in basalt (Wilshire and Binns, 1961). Olivine adjacent to xenolith margins commonly has a corona of small, colorless clinopyroxene rods, whereas clear apatite is converted to bluish-gray apatite without change in form.

Microfabric Analysis of Xenoliths

In an attempt to learn something of the conditions under which the xenoliths originated, the microfabric of several selected specimens was examined. The information available falls into two categories:

(i) details of the textural relations between grains, and (ii) patterns of lattice preferred orientation.

Patches and stringers of an interlocking mosaic consisting of all the constituents of the xenolith are well developed in peridotites, but are also found in gabbros and pyroxenites. The mosaics are located for the most part along the boundaries of large grains. Many grains of the mosaic, particularly of olivine and plagioclase, are equidimensional polygons which interlock perfectly with adjacent large grains (Fig. 2). A similar development of small polygonal grains has been observed in deformed peridotite masses (Yoshino, 1961, Plate XII, Fig. 3). Some bands of granular material cross single olivine grains, in which case the mosaic consists entirely of olivine in interlocking polygonal and anhedral grains (Fig. 3b). The mosaics occur along irregular fractures and are accompanied by slight external rotation of the two parts of the original grain. Green spinel in peridotite and gabbro xenoliths is concentrated in the granular mosaics where it may be graphically intergrown with clinopyroxene or olivine (Fig. 4). In feldspathic rocks, the granular mosaics rarely contain much plagioclase even where they occur along plagioclase

FIG. 2. Polygonal grains of olivine adjacent to a large strained olivine grain. Crossed polars (K29). Height of area 2.6 mm.

boundaries. In all xenolith types, the majority of olivine grains, including the rare euhedral grains, are cut by strain bands subparallel to {100} which divide single grains into zones with slightly different optical orientations. Fracturing along irrational planes has in some grains produced offsetting of strain bands. These bands have been called translation

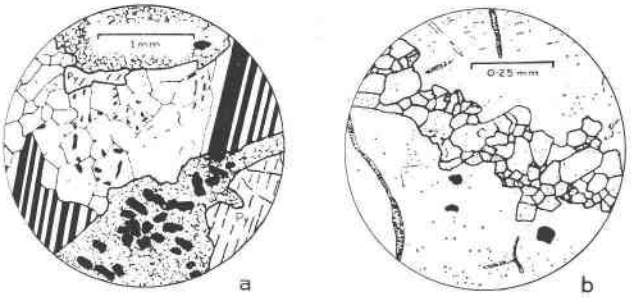

FIG. 3. (a) Clear grains of recrystallized plagioclase, some polygonal, between large original plagioclase grains (twinned). The matrix is fine-grained olivine (textured) and spinel (solid black). (K31). (b) Polygonal olivine grains cutting across a single large grain of olivine (K240).

lamellae (Ernst, 1936; Turner, 1942; Brothers, 1960; Wilshire and Binns, 1961), but as yet there is no evidence to support this interpretation and the bands are best called strain bands (Griggs *et al.* 1960, p. 54). The bands resemble strain shadows in quartz (Griggs *et al.*, 1960, p. 24). In contrast to the large grains, the polygonal grains in the granular mosaics

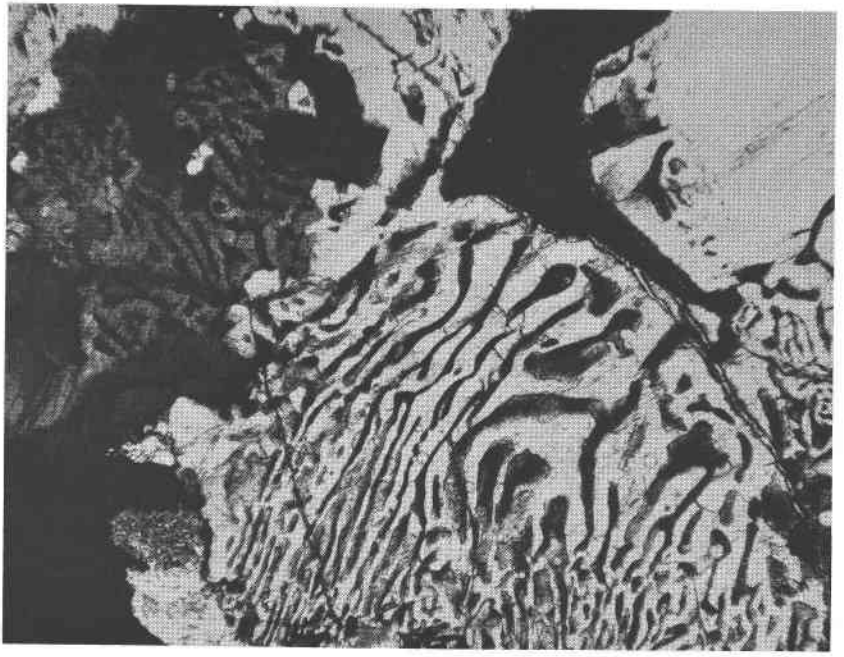

FIG. 4. Myrmekitic intergrowth of spinel and olivine (K31A). Width of area 2.9 mm.

do not show strain shadows although a few relicts of large strained olivines are found in the mosaics.

Kink bands are found in orthopyroxene and clinopyroxene (Fig. 1). The amount of external rotation illustrated in Fig. 1 is small but angles of up to 25° were measured. {100} planes have been externally rotated in clinopyroxene, but remain rational planes in the lattice. The axis of external rotation is [010]. Hence, following Turner (in Griggs *et al.*, 1960, p.

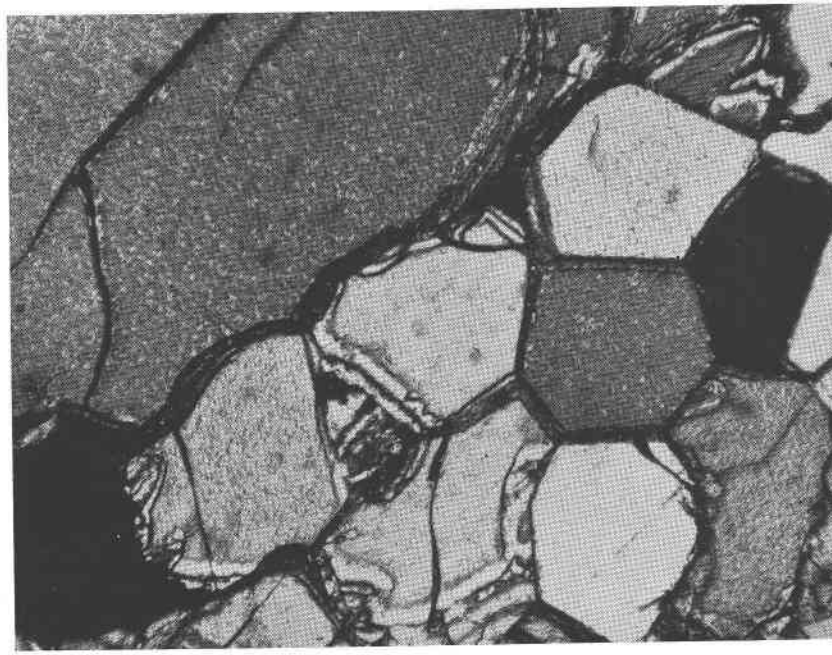

FIG. 5. Intergranular polygonal olivine grains between large strained olivine grains (K29). Width of area 2.9 mm.

60–61), the glide system in operation is: glide plane {100}, glide direction [001].

In other xenoliths where kinking of clinopyroxene is absent, signs of deformation are slight. Although exsolution lamellae of orthopyroxene parallel to {100} of the clinopyroxene are common, no evidence of slip such as internal rotation of planes inclined to [001] was found. In some grains slight warping of {100} planes has caused optical strain effects.

The orientation of X, Y and Z was determined on each of fifty grains of olivine in two peridotite xenoliths. In each case measurements were taken from only one section using a 4-axis universal stage and data were collected in two widely spaced traverses. Partial diagrams for twenty-five

grains are nearly identical for each section so that fifty grains appears to be adequate to show the major features.

The orientation diagrams for olivine of xenolith no. K44 (Figs. 6a, b, c) show that both X and Y occupy nearly coincident girdles perpendicular to a point maximum of Z. While the pattern is typical for olivine (Brothers, 1959, 1960), it is rare that such perfection in the pattern is developed and X rather than Z usually forms the point maximum (Battey, 1960, p.

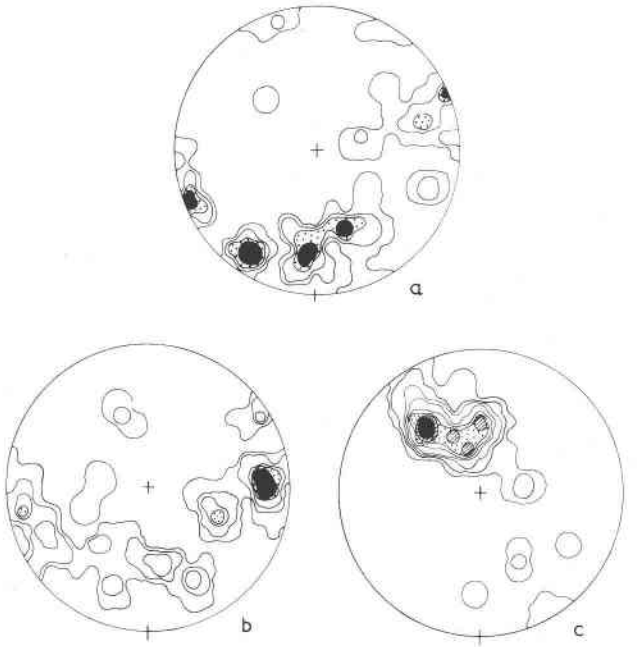

FIG. 6. (a) (b) (c) Orientation diagrams of X, Y and Z respectively in olivines from K44. Contours spaced at 2% intervals, *i.e.* 1, 3, 5 etc. per 1% area.

721). It should be emphasized that rod-shaped spinels of this xenolith, which occur along grain boundaries in the intergranular mosaic, have a preferred orientation which coincides with the Z point maximum of olivine. Such a fabric is similar to the fabrics developed in many tectonites (Battey, 1960). At present, there is no information regarding the mechanisms by which olivine deforms and develops a lattice preferred orientation so that the objections to this view raised by Brothers (1962) are without experimental support.

Xenolith no. K29 shows well developed granular mosaics along boundaries of large grains. The orientation diagrams for large olivines (Figs. 7a, b, c) show a more typical pattern with X tending toward a point maxi-

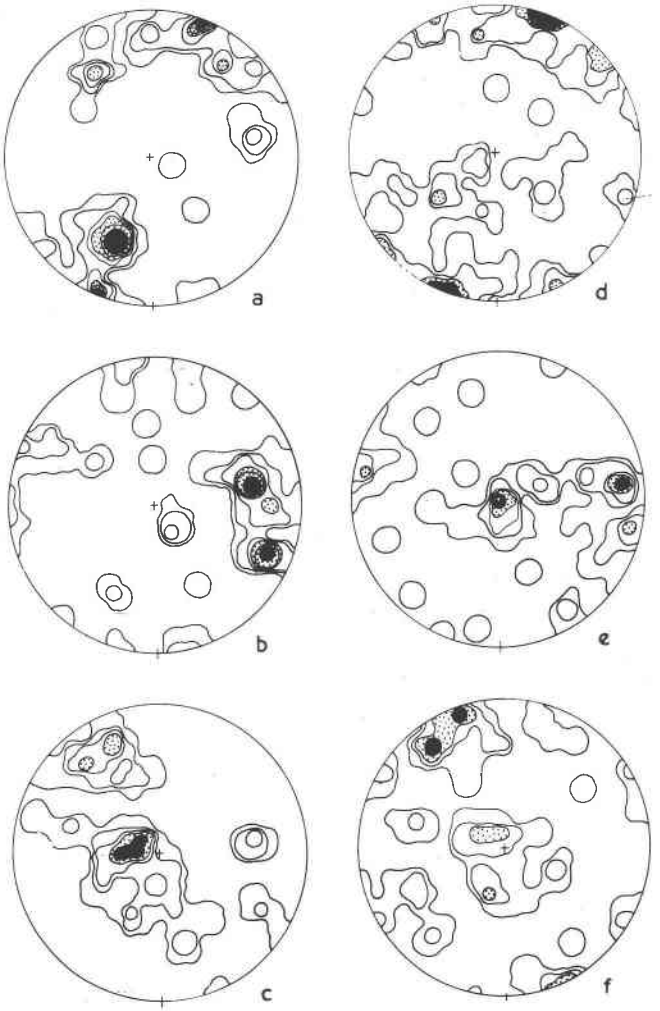

FIG. 7. (a) (b) (c) Orientation diagrams of X, Y and Z respectively in olivines showing strain in K29. (d) (e) (f) Orientation diagrams of X, Y and Z respectively in small polygonal olivine grains in K29. Contours as for Fig. 6.

mum, Y occupying a restricted area but spreading irregularly, and Z spreading in a girdle. Orientation diagrams for small polygonal grains in the same slide (Figs. 7d, e, f) show patterns similar to those of large grains. Yoshino (1961) shows a similar relation between the fabric of large and small grains in a deformed peridotite mass.

Additional orientation diagrams were prepared for clinopyroxene (Figs. 8a, b, c) and orthopyroxene (Figs. 8d, e, f) from a single biotite-horn-

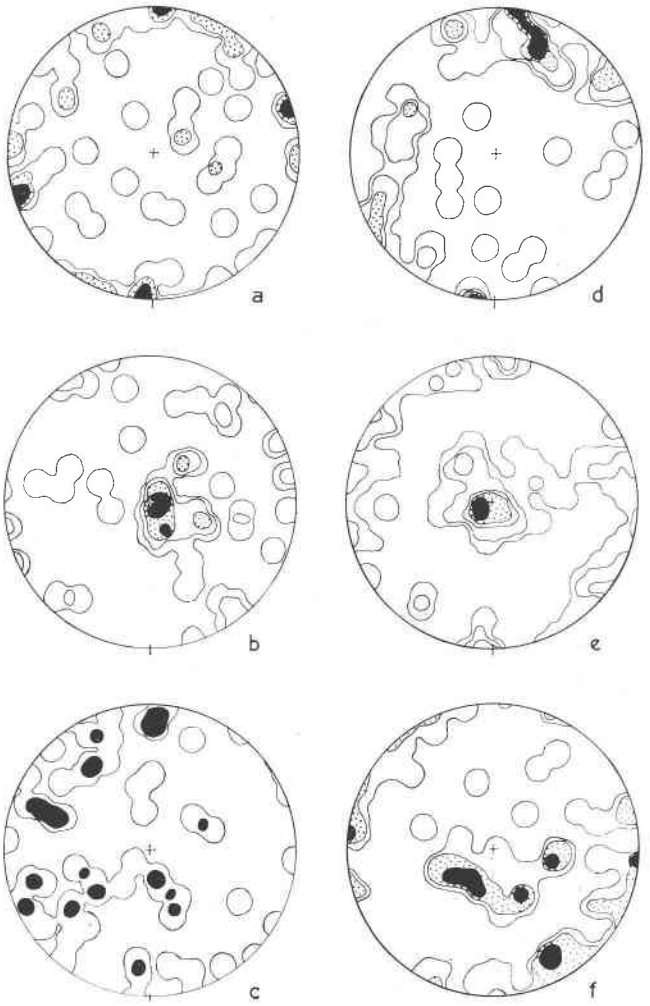

FIG. 8. (a) (b) (c) Orientation of X, Y and Z respectively in clinopyroxenes in K149. (d) (e) (f) Orientation of X, Y and Z in orthopyroxenes in K149. Contours as for Fig. 6.

blende pyroxenite xenolith (K149). This xenolith does not show signs of extensive deformation and many clinopyroxene grains are elongate. The clinopyroxene pattern is poorly developed with X forming a peripheral girdle but spreading irregularly over the remainder of the projection. Y forms a central maximum while Z is spread irregularly. Hypersthene patterns are better developed with X forming an oblique girdle, Y and Z forming central maxima which spread into weak peripheral girdles.

A review of olivine fabric types found in both deformed and unde-

formed rocks was presented by Brothers (1959); it was found that both viscous flow and solid deformation resulted in similar orientation patterns for olivine. Brothers (1960) rejected deformation as the mechanism of orientation of olivine in peridotite nodules from a basalt intrusion and considered the xenoliths to be of cognate, cumulative origin with orientation of olivine having been produced by convective deposition of crystals.

It is clear from Brothers' discussion (1959, pp. 577, 580) that an equidimensional habit of olivine is considered necessary to produce a preferred lattice orientation under conditions of viscous flow. Lacy (1960, p. 8) has pointed out that viscous flow in silicate melts must be a highly complex process involving continuous adjustment and modification of groups of molecules such as SiO_4 tetrahedra. Under such conditions, molecular configurations must develop which are stable under the particular conditions of viscous flow in operation. Thus, nuclei possessing quite definite lattice preferred orientations may be present long before crystallization has begun and this preferred orientation will be preserved in the final aggregate, with no direct genetical relation to the shape of the grains. Thus, on this basis, the presence or absence of an inequidimensional form of olivine grains need not be evidence for or against the development of lattice preferred orientation under conditions of viscous flow. However many of the patterns of preferred orientation recorded by Brothers (1959) are undoubtedly the result of orientation of inequidimensional grains in planes of laminar flow. Hence, the presence of a lattice preferred orientation in peridotite xenoliths is not sufficient evidence to distinguish between

(a) deformation in the solid state, (b) orientation due to grain shape during viscous flow, and (c) orientation of nuclei during viscous flow and their subsequent growth.

Details of the textures of the xenoliths studied furnish more data on the development of the fabrics of these rocks. The granular mosaics occurring between large grains are described by Brothers (1960, p. 72) as intercumulate precipitates composed in part of euhedral olivine. That this is not the origin of the granular mosaics in Kerguelen xenoliths is suggested by the occurrence of these mosaics along fractures in large grains (Fig. 3), by a preferred orientation of mosaic constituents identical with that of large grains, and by parallelism between rod-shaped spinels isolated within the granular mosaic and the Z point maximum of large grains in xenolith no. K44. Nothing approaching this type of fabric was described by Wager *et al.*, (1960) or Jackson (1961) as resulting from intercumulate precipitation. The small polygonal grains of the granular mosaics are not properly described as "euhedral" since the bounding faces are often irrational and strongly curved. The same grain shapes are developed by

plagioclase (Fig. 3a), pyroxene and olivines. Further, most grains are arranged so that three grain boundaries meet, in section, at a point where interfacial angles close to 120° are developed or approached by curvature of grain boundaries. Such features are conclusive evidence that these aggregates have undergone adjustment of grain boundaries in the solid state under the influence of interfacial (solid-solid) energy. See McLean (1957, pp. 81–92) for a discussion of such features. The further observation that these polygonal aggregates possess a lattice preferred orientation similar to that of the large grains implies that these grains have originated by recrystallization. Thus, the granular mosaics are interpreted as products of recrystallization of the plastically deformed crystal aggregate, with nucleation having taken place in the loci of high strain in the aggregate, namely, along boundaries of grains which have undergone relative external rotation and in highly strained parts of single grains. This is analogous to experimentally deformed metals where recrystallized grains tend to develop in sites where the strain is localized. Such locations include slip planes, twin boundaries, and grain boundaries, and in general the recrystallized mosaic has an orientation which bears some clear relationship to that of the host material (Burke and Turnbull, 1952). Similar effects have been observed in experimental recrystallization of calcite aggregates under stress (Griggs *et al.*, 1960, p. 94–97). The resemblance of strain bands in the large olivines to undulatory extinction bands in quartz suggests that these may be due to polygonization during the recovery process following deformation (Griggs *et al.*, 1960, p. 24).

Hence, although the existence of a lattice preferred orientation in these rocks offers little information on their origin, there is some evidence in the textural relations that the xenoliths have undergone some deformation and subsequent grain boundary adjustments in the solid state.

Xenocrysts

Phenocrystal constituents of basalts and oceanites are dominantly subhedral or euhedral olivine and salite. Xenocrystal olivine is distinguished from phenocrysts by the presence of deformation lamellae and general lack of crystal faces in xenocrysts. As clearly shown at xenolith margins, clinopyroxene xenocrysts react readily with the magma to form salite and further crystallization from the host magma may change anhedral xenocrysts to euhedral crystals identical with phenocrysts; hence, clinopyroxene can be identified as xenocrysts only where ragged cores of colorless or green clinopyroxene ($\beta = 1.694$–1.695, $2V_z = 51°$–$56°$) are preserved and by the uncommon preservation of orthopyroxene exsolution lamellae in such cores. Orthopyroxene is not an intratelluric mineral in alkali basalts (Wilkinson, 1956) and all grains have coronas of granular

olivine which is the characteristic reaction product of orthopyroxene at margins of xenoliths. Green and brown spinel grains with opaque rims are interpreted as xenocrysts because conversion to an opaque mineral is the same as the reaction found at xenolith margins; these anhedral xenocrysts are commonly very large compared to euhedral opaques crystallized from the host magma.

Classification of Kerguelen rocks is to a large extent dependent on the amount of xenocrystal material present. Thus, oceanites and limburgites generally contain a high proportion of xenocrysts derived from peridotite; were this material removed, the host rocks would have a composition similar to that of ordinary basalts. The amount of foreign material decreases from limburgites through basalts to ophitic basalts and hawaiites. The proportions of xenocrystal minerals, however, are not in keeping with the proportions of the same minerals in xenoliths, both orthopyroxene (or reaction products) and plagioclase being far less abundant as xenocrysts than as constituents of xenoliths. Perhaps partial fusion of rocks similar to the xenoliths first affected orthopyroxene and plagioclase causing disaggregation of olivine and clinopyroxene which appear as xenocrysts.

Chemistry of the Olivines

Published analyses of olivines from peridotite nodules in basalts vary within narrow limits (*e.g.* 8.61 to 10.26% FeO from Ross *et al.*, 1954). Olivine from basic rocks show a more variable and higher FeO content (Deer *et al.*, 1962), suggesting that xenocrysts, if derived from xenoliths, would have a different composition from phenocrysts.

To test this hypothesis, partial analyses were done on sixteen olivines from xenoliths, eleven xenocrystal olivines and twelve phenocrystal olivines. Data on three olivines from the Crozets (Tyrrell, 1937) are included for comparison, since the Crozet rocks are similar to those of Kerguelen.

Techniques of separation and analysis. The separations were carried out with heavy liquids and by use of a Franz isodynamic separator. Final separation was achieved by hand picking, care being taken to remove all grains with inclusions. Contamination with groundmass olivine was minimized by using only the $-60+85$ B.S.S. fraction where possible. However, analyses of different sieve fractions did not yield significantly different results. Iron, cobalt, nickel and manganese were chosen for analysis since these elements are the most significant elements in the analyses of Ross *et al.* (1954).

X-ray fluorescent analysis techniques were used for the determination

of iron, nickel and manganese. Although it was intended to analyze for cobalt, the "trace" amounts of it in the presence of large quantities of iron meant that the CoKα line (1.791 Å) was not resolved from the FeKβ_1 line (1.757 Å). It was not found practicable to use other cobalt lines.

All analyses were made using a focussing spectrograph designed by Norrish and Radoslovich (to be published). A curved LiF crystal cut parallel to the 200 plane (d = 2.01 Å) was used as the analyzing crystal for the iron and nickel determinations. The $10\bar{1}1$ plane (d = 3.343 Å) of quartz was used in the case of manganese.

A Raymax demountable self-rectifying *x*-ray tube was the source of the primary radiation. The targets used, electroplated from high purity reagents, and the operating conditions for the three elements are listed below:

Fe analysis: Cu Target, 50 K.V., 25 mA.
Ni analysis: Au Target, 50 K.V., 20 mA.
Mn analysis: Co Target, 40 K.V., 17.5 mA.

Counts from samples were registered by means of a scintillation detector and associated electronic apparatus. This apparatus included a linear amplifier and pulse height analyzer. About 40 mgms of olivine was used for analysis. The techniques used for the determination required the measurement of the mass absorption coefficients of the samples. The samples were therefore prepared by pressing the finely ground powder into a 0.95 cm diameter hole in a "Perspex" holder. No binder material was necessary. Samples of uniform thickness were obtained by the use of jigs.

The olivines were analyzed for nickel and manganese using a combination of monochromatic *x*-ray absorptiometry and fluorescent *x*-ray spectrography essentially similar to that outlined by Salmon and Blackledge (1956). Measurement of fluorescent intensity involved a count on both the line (NiKα = 1.659 Å, MnKα = 2.103 Å) and a background. Standards were run at frequent and regular intervals to correct for any variations in instrumental conditions.

The percentage error for the relatively low nickel and manganese (20 to 300 ppm), where the limit of detection is fixed by counting statistics, was less than three per cent. For higher amounts of these two elements the error was fixed by absorption measurements and was again less than three per cent.

The technique used for the determination of iron was basically a calibration curve. This was possible because, although olivines are not a two component system, the iron, magnesium and silicon are highly correlated. The relative percentage error in these determinations was less than one per cent.

TABLE 1. PARTIAL ANALYSES OF OLIVINES

Group 1. Olivines from xenoliths

	1	2	3	4	5	6	7	8	9	10	11	12	13	14	15	16
FeO	10.2	8.15	8.44	13.45	18.0	8.36	8.95	12.2	11.8	16.3	13.6	9.23	9.25	13.7	14.7	14.4
Ni	0.282	0.254	0.281	0.260	0.186	0.295	0.308	0.245	0.298	0.195	0.227	0.288	0.314	0.221	0.222	0.292
Mn	0.14	0.11	0.12	0.18	0.20	0.12	0.12	0.17	0.16	0.20	0.18	0.12	0.12	0.16	0.16	0.18

Group 2. Xenocryst olivines

	17	18	19	20	21	22	23	24	25	26	27
FeO	9.07	21.0	14.6	14.5	13.8	13.9	16.9	16.8	18.8	16.3	16.1
Ni	0.301	0.123	0.218	0.184	0.244	0.206	0.219	0.206	0.195	0.234	0.170
Mn	0.12	0.30	0.20	0.18	0.16	0.18	0.23	0.20	0.24	0.20	0.20

Group 3. Phenocryst olivines

	28	29	30	31	32	33	34	35	36	37	38	39
FeO	22.7	19.0	21.2	18.9	18.8	23.3	20.1	24.5	26.5	26.3	27.4	26.0
Ni	0.076	0.124	0.195	0.139	0.128	0.095	0.150	0.140	0.092	0.064	0.118	0.097
Mn	0.34	0.30	0.36	0.24	0.24	0.32	0.25	0.31	0.38	0.39	0.38	0.34

The results of the analyses are shown in Table I and in Fig. 9. The locations of samples is given in Table II. The analyses for iron are given as FeO to facilitate comparison with other published data although no ferrous iron determinations were carried out.[1]

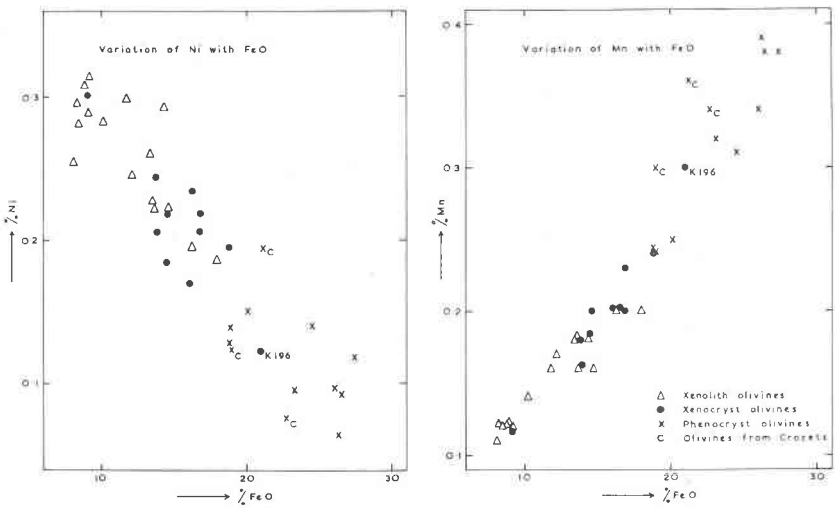

FIG. 9. Variation diagrams of Ni and Mn against FeO.

[1] Fifteen analyses of olivines performed by M. D. Foster (Ross *et al.*, 1954) showed only one with any Fe_2O_3 and this one only 0.30%.

TABLE 2. LOCALITIES OF SAMPLES

Sample No.	BANZARE No.	Location and description	(Mawson's catalogue)
1	K26	Royal Sound, Kerguelen Is.	Olivine nodule in basalt.
2	K29A sample a	"Nodule locality" behind Jeanne d'Arc.	Isolated nodule.
3	K29A sample b	"Nodule locality" behind Jeanne d'Arc.	Isolated nodule.
4	K29C	Locality C. Kerguelen Is.	Olivine nodule in basalt.
5	K30 f.gd.xen.	Locality C. Kerguelen Is.	Olivine nodule in basalt.
6	K30 c.gd.xen.	Locality C. Kerguelen Is.	Olivine nodule in basalt.
7	K30*[1]	Locality C. Kerguelen Is.	Olivine nodule in basalt.
8	K30A c.gd.xen.	Locality C. Kerguelen Is.	Olivine nodule in basalt.
9	K30A m.gd.xen.	Locality C. Kerguelen Is.	Olivine nodule in basalt.
10	K30B	Locality C. Kerguelen Is.	Olivine nodule in basalt.
11	K30C f.gd.xen.	Locality C. Kerguelen Is.	Olivine nodule in basalt.
12	K30C c.gd.xen.	Locality C. Kerguelen Is.	Olivine nodule in basalt.
13	K32	Locality C. Kerguelen Is.	Olivine nodule in basalt.
14	K44	Main hill of Murray Is.	Isolated nodule.
15	K248	Schum Is. (Royal Sound).	Olivine nodule in basalt.
16	K249	SE. corner, bay of Schum Is. Boulder on beach.	Olivine nodule in basalt.
17	K41	Royal Sound, Kerguelen Is.	Basalt.
18	K196	Port Phonolite, Greenland Harbor, Kerguelen Is.	Oceanite.
19	K204	South slopes at spit at head of Bras Bolinder, Kerguelen Is.	Oceanite.
20	K206	South slopes at spit at head of Bras Bolinder, Kerguelen Is.	Oceanite.
21	K240	Schum Is.	Oceanite.
22	K242	Schum Is.	Basalt.
23	K245	Schum Is.	Basalt.
24	K246	Schum Is. Boulder on beach.	Basalt.
25	K247	Schum Is.	Basalt.
26	K249	Schum Is. Boulder on beach.	Oceanite.
27	K283	Murray Is. anchorage. Moraine boulder derived from vicinity of Mt. Wyville Thompson.	Oceanite.
28	C7	Possession Is., Crozets. W. side American Bay.	Ankaramite.
29	C9	Possession Is., Crozets. S. headland of American Bay.	Basalt.
30	C22	Possession Is., Crozets. Boulder W. side of American Bay.	Basalt.

TABLE 2.—(*Continued*)

Sample No.	BANZARE No.	Location and description	(Mawson's catalogue)
31	K60	Murray Is. anchorage. E. end of Long Is.	Ophitic Basalt.
32	K61	Murray Is. anchorage. N. end of lake on Long Is.	Ophitic Basalt.
33	K88	Graves Is. (Royal Sound).	Basalt.
34	K130	Jeanne d'Arc. Boulder in creek.	Ophitic Basalt.
35	K134	Jeanne d'Arc. Boulder in creek.	Ophitic Basalt.
36	K142	Jeanne d'Arc. Boulder in creek.	Hawaiite.
37	K183	Jeanne d'Arc from 30′ basalt flow 130′ O.D.	Ophitic Basalt.
38	K201	Spit at head of Bras Bolinder. Moraine boulder.	Basalt.
39	K307	Mt. Wyville Thompson. Two-thirds way up to slope.	Trachybasalt.

Discussion of analyses. Ross *et al.*, (1954) in a study of dunite nodules in basalt from many localities found that the range in composition of the olivines varied between 8.15 and 10.2% FeO; 0.23–0.37% Ni; and 0.09–0.13% Mn.[1] Seven of our analyses of nodule olivines fall within this range. However, these with the other nine analyses establish a trend with Ni diminishing to 0.18% and FeO and Mn increasing to 18% and 0.2% respectively.

The xenocryst olivines fall mainly within the range of variation of the xenolith olivines but tend to be richer in FeO and Mn and poorer in Ni (Fig. 9). The range of values for the phenocryst olivines falls outside that of the other two groups.

All the analyzed samples of xenocryst olivines contained variable amounts of phenocryst olivines, even though the specimens from which the olivines were separated were chosen on the basis of having a high ratio of xenocryst to phenocryst olivine.[2] It is impossible to distinguish between xenocryst and phenocryst olivine while handpicking the crushed and separated sample. This contamination would tend to displace the composition in the direction of increasing FeO and Mn and decreasing Ni. This suggests that there is no significant difference in composition

[1] Mean of "classical" and spectrographic determinations.

[2] K196 shows a fair proportion of phenocryst olivine in thin section and this may account for its apparent anomalous composition.

between the xenolith and xenocryst olivines. The phenocryst olivines on the other hand form another group quite distinct from the xenolith olivines. These results are consistent with the hypothesis that the xenocrysts are derived from the xenoliths and that the phenocrysts have an origin different from that of the xenocrysts.

The graphs of Fig. 9 show that the trends of the composition of the phenocryst and xenocryst olivines appear to be related.[1] However the trends shown by our analyses are similar to those shown by the published analyses (see Vogt, 1923; Goldschmidt, 1929; Wager and Mitchell, 1951) in spite of differences in origin and geographical distribution. This suggests a common controlling mechanism for the distribution of Ni and Mn in olivines (see Ringwood, 1955, 1956, for a discussion of the structural control of Ni in olivines). In view of these arguments we feel that the relationships in the trends of composition of the xenocryst and phenocryst olivines does not necessarily imply any simple genetic relationship.

Origin of Xenoliths

The two most commonly accepted theories of the origin of peridotite xenoliths in volcanic rocks (Wilshire and Binns, 1961), are: 1) cognate xenoliths derived from early formed differentiates of the host rock, and 2) relicts of the mantle rock from which the basalts have been derived by partial fusion.

A cognate origin of Kerguelen xenoliths is supported by the nearly complete continuity of mineral composition from xenoliths through xenocrysts to phenocrysts of the host rocks, and by the nearly complete restriction of alkaline xenoliths to trachybasalt host rocks. A mantle origin is favored by the occurrence in xenoliths of orthopyroxene which is not a product of intratelluric crystallization from alkali basalt host rocks (Wilkinson, 1956), and by intergranular, recrystallized mosaics and pyroxene-spinel intergrowths which have no counterparts in common cumulative rock fabrics.

The features favoring a mantle origin can be reconciled with a cognate source if it is assumed that orthopyroxene can crystallize from alkali basalt magma at very high pressure. Local deformation of cumulative rocks has produced several of the deformation features so common in

[1] Regressions of FeO(Y) on Ni(X_1) and Mn(X_2) were calculated for the three groups of analyses. The regression planes were not significantly different so the data from the three groups were pooled and the following regression equation obtained:

$$Y = 11.24 - 24.43X_1 + 45.83X_2$$

The root mean square deviation from regression is 1.381, both regression coefficients being highly significant ($p < .01$). The multiple correlation coefficient is 0.97. Statistical analysis by N. S. Stenhouse, Div. of Math. Stat., C.S.I.R.O., Adelaide.

xenoliths (see, for example, Jackson, 1961, p. 18), and deformation fabrics identical with those described here are found in the Twin Sisters dunite intrusion in Washington (D. M. Ragan, personal communication) though such rocks are not necessarily cumulative types. In any event it is entirely possible that solid deformation producing the structures observed in xenoliths could accompany some filter-press mechanism for removal of interstitial, basaltic, liquids from cumulative rocks.

Although the range of olivine compositions from Kerguelen xenoliths is unusually large, the range in rock types is also unusually great. If it is assumed that this range of rock types, from dunite through feldspathic peridotite to gabbro, represents variation in mantle composition, the continuity of olivine compositions from xenoliths and xenocrysts to phenocrysts need not preclude a mantle origin of xenoliths. Likewise, restriction of alkaline xenoliths to trachybasalt host rocks is not completely opposed to a mantle origin, for this relation is not found in other provinces (Wilshire and Binns, 1961), and examples have been reported of biotite and hornblende reaction rims on dunite xenoliths (Taylor, 1958, p. 68).

From the foregoing discussion it is evident that the data at hand are not adequate to distinguish between a cognate or a mantle origin of the xenoliths.

Acknowledgments

The authors wish to thank the committee of the Mawson Institute of Antarctic Research for permission to work on specimens housed in the Institute. We wish to thank Drs. K. Norrish, J. B. Jones and A. W. Kleeman for helpful discussion of the results.

Wayne K. Harris and Miss C. Miller did much of the tedious work on the preparation of the samples for analysis. Miss M. Swan prepared the line figures for publication.

References

Battey, M. H. (1960) The relationship between the preferred orientation of olivine in dunite and the tectonic environment. *Am. Jour. Sci.* **258,** 716–727.

Brothers, R. N. (1959) Flow orientation of olivine. *Am. Jour. Sci.* **257,** 574–584.

——— (1960) Olivine nodules from New Zealand. *Intl. Geol. Cong. Reports, 21st Sess. Pt.* **13,** 68–81.

——— (1962) The relationship between preferred orientation of olivine in dunite and tectonic environment. *Am. Jour. Sci.* **260,** 310–312.

Burke, J. E. and D. Turnbull (1952) Recrystallization and grain growth. *Prog. in Met. Phys.* **3,** 220–292.

de la Rue, A. (1932) Étude geologique et geographique de l'Archipel de Kerguelen. *Rev. Geog. Physique Geol. Dynamique.*

Deer, W. A., R. A. Howie and J. Zussman (1962) *Rock Forming Minerals. Vol. 1. Ortho- and Ring Silicates.* Longmans.

EDWARDS, A. B. (1938) Tertiary lavas from the Kerguelen Archipelago. *BANZARE Reports, Ser. A*, **2**, 69–100.

ERNST, T. (1936) Olivinknollen der Basalte als Bruchstücke alter Olivinfelse. *Nachr. Gesell. Wiss. Göttingen, Math-Phys. K1, Gp. IV*, **1**(13), 147–154.

FRECHEN, J. (1948) Die Genese der Olivinausscheidungen von Dreiser Weiher (Eifel) und Finkenberg (Siebengebirge) *Neues Jahrb. Min. Geol. Pal.* **79**, 317–406.

GOLDSCHMIDT, V. M. (1929) Die Naturgeschichte der Eisenfamilie. *Stahl und Eisen*, **49**, 601–612.

——— (1954) *Geochemistry* (Ed. A. Muir). Oxford University Press.

GRIGGS, D. AND J. HANDIN (ed.) (1960) Rock Deformation. *Geol. Soc. Am. Mem.* **79**.

HOLMES, A. AND H. F. HARWOOD (1937) The petrology of the volcanic area of Bufumbira. *Mem. Geol. Surv. Uganda* **3** (2).

JACKSON, E. D. (1961) Primary textures and mineral associations in the ultramafic zone of the Stillwater Complex, Montana. *U. S. Geol. Surv. Prof. Paper*, **358.**

LACY, E. D. (1960) Melts of granitic composition: their structure, properties and behavior. *Intl. Geol. Cong., 21st Sess., Pt.* **14**, 7–15.

MCLEAN, D. (1957) *Grain Boundaries in Metals*. Clarendon Press, Oxford.

RINGWOOD, A. E. (1955) The principles governing trace element distribution during magmatic evolution. Part I. The influence of electronegativity. *Geochim. Cosmochim. Acta*, **7**, 189–202.

——— (1956) Melting relationships of Ni-Mg olivines and some geochemical implications. *Geochim. Cosmochim. Acta*, **10**, 297–303.

ROSS, C. S., M. D. FOSTER AND A. T. MYERS (1954) Origin of olivine-rich inclusions in basaltic rocks. *Am. Mineral.* **39**, 693–737.

SALMON, M. L. AND J. P. BLACKLEDGE (1956) A review of improved mineral analyses by fluorescent *x*-ray spectrography. *Norelco Rept.* **3**, 68, 73.

TAYLOR, G. C. (1958) The 1951 eruption of Mount Lamington, Papua. *Australia Bur. Min. Res. Bull.* **38.**

TURNER, F. J. (1942) Preferred orientation of olivine crystals in peridotites, with special references to New Zealand examples. *Trans. Roy. Soc. New Zealand*, **72**, 280–300.

TYRRELL, G. W. (1937) The petrology of Possession Island. *BANZARE Reports, Ser. A*, **2**, (4) 57–68.

VOGT, J. H. L. (1923) Nickel in igneous rocks. *Econ. Geol.* **18**, 307–353.

WAGER, L. R., G. M. BROWN, AND W. J. WADSWORTH (1960) Types of igneous cumulates. *Jour. Petrol.* **1**, 73–85.

——— AND R. L. MITCHELL (1951) The distribution of trace elements during strong fractionation of basic magma. *Geochim. Cosmochim. Acta*, **1**, 129–208.

WILKINSON, J. F. G. (1956) Clinopyroxenes of alkali olivine-basalt magma. *Am. Mineral.* **41**, 724–743.

WILSHIRE, H. G. AND R. A. BINNS (1961) Basic and ultrabasic xenoliths from volcanic rocks of New South Wales. *Jour. Petrol.* **2**, 185–208.

YOSHINO, G. (1961) Structural-petrological studies of peridotite and associated rocks of the Higashi-Akaishi-Yama district, Shikoku, Japan. *Jour. Sci. Hiroshima Univ. Ser. C*, **3**, 343–402.

Manuscript received, November 15, 1961; accepted for publication, November 1, 1962